Fe-supported perlite applied for the degradation of Rhodamine B dye by Heterogeneous Fenton reaction

Jessica Oliveira Aguiar Perez[a], Gabriela Tuono Martins Xavier[a], Gustavo Felix Bitencourt[a]
Luana dos Santos Andrade[a], Wagner Alves Carvalho[a], Yvan Jesus Olortiga Asencios[a,b]
[a] *Universidade Federal do ABC (UFABC), Av. Dos Estados, 5001, Santo André, São Paulo, Brasil*
jessica.perez@ufabc.edu.br
[b] *Universidade Federal de São Paulo (UNIFESP), Rua Dona Maria Máximo, 168, Ponta da Praia, Santos, SP, Brasil*
yvan.jesus@unifesp.br

DOI: https://doi.org/10.34024/jsse.2024.v2.19444

Abstract*— This study aimed to evaluate a technique of Fe ion impregnation on perlite mineral and assess its behavior in a heterogeneous Fenton-like reaction, at room temperature and under acidic and alkaline conditions in the removal of Rhodamine B dye. For the catalyst preparation, a suspension of heptahydrated ferrous sulfate ($FeSO_4.7H_2O$) was used, followed by thermal treatment (calcination). Different doses of H_2O_2 (35% v/v) were applied to evaluate dye removal rates. Fe leaching in reaction media was analyzed. The percentages were 36.1%, 25.5%, 36.5%, 14.9%, 13.5%, and 29.8% for reactions at initial pH values of 4, 7, 9, 10, 11, and 12, respectively. Rhodamine B removal at pH 4, 7, 9, 10, and 11 had the respective removal rates of 99.8%, 57.4%, 73.1%, 77.5%, and 96.9% in 240 minutes of reaction. At pH 12, there was 99.7% removal in 110 minutes of reaction. Reactions performed with low dosages of hydrogen peroxide showed, at pH 4 and 11, removal percentages of 95.8% and 90.2%, respectively, in 150 minutes of reaction. Under the same conditions, at pH 12, the removal percentage was 98.6% in 105 minutes. The synthesized catalyst exhibited satisfactory activity under acidic and alkaline conditions, for three cycles, showing promise for applications in heterogeneous Fenton reactions on a large scale.

***Keywords*— Heterogeneous Fenton, Perlite, Rhodamine B,**

I. INTRODUCTION

The Sustainable Development Goals (SDGs) address issues related to potable water availability and sustainable wastewater treatment proposals. Dyes are used by industrial sectors in diverse areas in their products, resulting in their discharge into water resources. The presence of dyes in water bodies triggers environmental pollution problems due to their high stability arising from their chemical structures, offering resistance to degradation [1]. Figure 1 shows the molecular structure of Rhodamine B (RhB), which is a cationic xanthene dye that is bright reddish-pink and highly soluble in water [2].

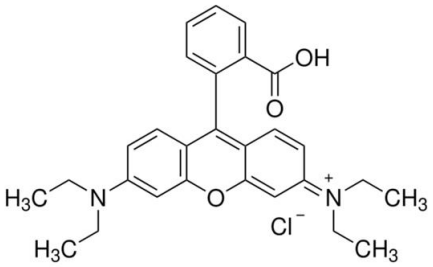

Fig. 1. Molecular structure of Rhodamine B.

Used in the textile, plastic, printing, biomedical, and leather industries, RhB is commonly employed as a dyeing agent, photosensitizer, fluorescent marker for microscopic analysis, and biological dye in biomedical research [3]. Rhodamine B (RhB) poses a significant environmental and human health threat. In aquatic animals, RhB causes respiratory damage, tissue necrosis, and reproductive problems. In severe cases, human exposure can lead to cancer and genetic mutations. Ingestion of this substance is toxic and irritates the skin, eyes, and respiratory system. RhB is difficult to biodegrade, which contributes to persistent environmental pollution. The presence of RhB in water bodies harms aquatic organisms, as it interferes with the penetration of sunlight necessary for algal photosynthesis [4]. Therefore, industries that use RhB must implement efficient effluent treatment systems to completely remove the dye before discharging it into the aquatic environment. This measure is fundamental to protecting aquatic ecosystems and human health [3].

One of the solutions proposed for treating this type of effluent is Advanced Oxidation Processes (AOPs), defined as oxidation processes that involve the generation of radicals in sufficient quantities to allow the oxidation of a large number of organic pollutants [5]. Among such processes, there are Fenton oxidation processes, applied in the treatments of a wide variety of organic molecules in aqueous media. The active sites in the Fenton process are iron ions that catalyze the breakdown of hydrogen peroxide molecules into hydroxyl radicals. Figure 2 shows the formation of aromatic intermediates generated during the degradation of Rhodamine B (RhB) after the removal of its external functional groups. RhB has phenylamino and carbonyl groups, responsible for its coloration due to the presence of C=N and C=O bonds [6].

In the reaction, the generated hydroxyl radicals (•OH) attack the central carbon of RhB, triggering N-deethylation and subsequent decolorization of the dye. Mass spectral analysis reveals the presence of intermediates such as: N,N-diethyl-N-ethyl-rhodamine (m/z 443); N,N-diethyl-rhodamine (m/z 415); N-ethyl-rhodamine (m/z 387) and intermediates with m/z 359 and 274. With the gradual breakdown of RhB's conjugated structures, the benzene rings open, forming aromatic ring molecules such as: $C_{13}H_{13}N_2O^+$ (m/z 213) and $C_{17}H_{13}O$ (m/z 230). These intermediates undergo further oxidation, generating small molecule acids such as Phthalic acid (m/z 166) 3,4-dihydroxybenzoic acid (m/z 155). Finally, the small organic molecules are mineralized by •OH, converting to NO^{3-}, NH^{4+}, CO_2 and H_2O. This detailed analysis of RhB degradation intermediates by photo-Fenton offers a complete overview of the process, from initial decolorization to final mineralization, highlighting the method's effectiveness in removing organic dyes [6].

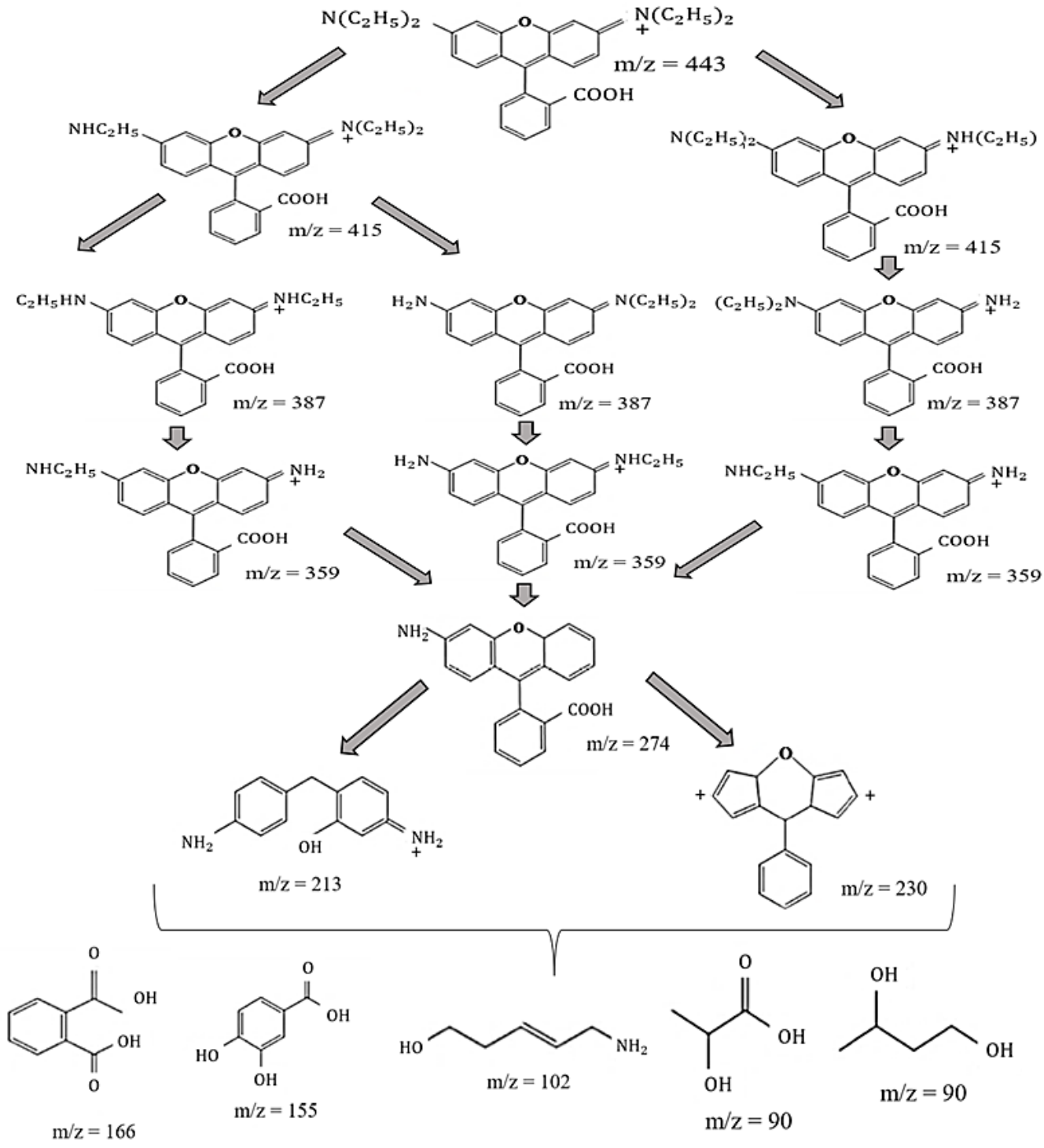

Fig. 2. Mechanism of Rhodamine B degradation [6].

The application of Fenton processes extends to various types of effluents and the applied catalysis is typically homogeneous, generating some drawbacks such as sludge generation, besides requiring acidified reaction media for satisfactory catalytic performance, necessitating pH adjustments before the reaction starts, consuming non-reusable reagents. In this way, it is necessary to make heterogeneous Fenton processes viable, in which a solid catalyst is used as a source of iron, instead of ferrous ions as in homogeneous Fenton processes, seeking catalysts that operate in a wide pH range, in order to avoid the consumption of reagents in adjustments of reaction media for restricted conditions. The recovery of the solid catalyst ensures a clean final solution and its reuse after multiple uses [7].

Synthesis of heterogeneous catalysts has involved metals supported on surfaces that, in general, have good adsorbent capacity, due to their large surface area. The search for efficient adsorbents for the removal of contaminants has driven research in various areas, including synthetic and natural adsorbents. Natural adsorbents, such as those derived from seeds, cereal residues (e.g., wheat straw), coconut shells, sugarcane bagasse and fruits, as well as minerals such as clay and zeolite, have gained prominence due to their availability and potential for superior performance. The abundance and low cost of these materials, coupled with growing concerns about sustainability, are driving scientists to continuously explore the potential of natural adsorbents for the removal of contaminants, seeking efficient and environmentally friendly alternatives for environmental protection [8].

Reference [9] synthesized bimetallic Fe-Cu catalysts supported on biochar using a pyrolysis method with waste generated from the paper and pulp industry. They utilized Fenton process sludge as the iron source, acid-precipitated black liquor as the carbon source, and copper nitrate as the copper source. The catalyst was applied in a Fenton reaction, achieving complete removal of 10 ppm RhB within 60 minutes under acidic conditions (pH 3, 0.2 g/L catalyst, and 1 mM H_2O_2) and within 6 hours at neutral pH (pH 7, 0.25 g/L catalyst, and 25 mM H_2O_2). Reference [10] synthesized amino-functionalized iron-based MOFs and applied them in a photo-Fenton reaction for the degradation of RhB. The material exhibited 90% removal of the dye after five consecutive degradation experiments, demonstrating effective performance over a wide pH range (3.0–7.0). Reference [11] synthesized a visible light-responsive, narrow band gap, heterogeneous photo-Fenton catalyst composed of micronized γ-Fe_2O_3/CQDs. The photo-Fenton catalytic degradation of γ-Fe_2O_3/CQDs in dye solutions, including Rhodamine B (RhB), Methylene Blue (MB), and Methyl Orange (MO), was investigated and compared to the activity of α-Fe_2O_3. Results showed that the γ-Fe_2O_3/CQDs material exhibited significantly superior catalytic performance for the degradation of various dyes, with a first-order rate constant (k) 14 times higher than that of α-Fe_2O_3, using a low H_2O_2 concentration (0.049 mmol/L) and a wider pH range (3.1–7.1). Reference [12] synthesized an efficient octahedral Fe_3O_4 oxide-graphene (OFe-GO) nanocomposite, magnetically separable, and applied it in a Fenton reaction for the complete degradation of Rhodamine B (50 mg/mL) within 15 minutes of reaction time. Reference [13] removed Rhodamine B using heterogeneous Fenton reaction using granular catalysts synthesized by incorporating Fe into attapulgite clay. The dye removal remained above 98% for 5 cycles of catalyst reuse.

Expanded perlite, also known as volcanic glass, is a material composed mainly of silica (SiO_2) and alumina (Al_2O_3), with approximately 75% and 14% of its composition, respectively. Its production involves crushing the raw material, perlite ore, and heating. Expanded perlite has a porous structure, which makes it a lightweight glass material with superior physical properties. Its characteristics include its applications as thermal insulation, insulation for flame and chemicals, and filtration aid, similar to diatoms. Expanded perlite is a versatile material with applications in various areas, due to its lightness, resistance and insulating properties [14]. Reference [15] developed a composite catalyst of Fe_2O_3 in expanded perlite (PE) for the degradation of Rhodamine B (5 mg/L) in a heterogeneous photo-Fenton system, using H_2O_2 and visible light irradiation. According to the referred study, the Fe_2O_3/PE catalyst demonstrated high efficiency in the degradation of Rhodamine B over a wide pH range (2 to 10). Under the best experimental conditions (0.5 g/L of catalyst and 2 mL/L of H_2O_2), a degradation rate of 99% and a COD removal rate of 62% were achieved in 90 minutes. In the same study, Iron leaching from the catalyst during the reaction was minimal, indicating its high stability. After five cycles of use, the catalyst still exhibited high catalytic activity, proving its reusability and potential for practical applications. The high porosity and chemical inertness of expanded perlite make it an ideal support for the Fe_2O_3 catalyst, providing an efficient contact surface for the reaction and ensuring the stability of the catalyst during the process. Reference [16] grafted expanded perlite and red ochre onto SCN-doped gC_3N_4, producing a photocatalyst active in the removal of methylene blue and the decontamination of Total Organic Carbon (TOC), achieving removals of 99.6% and 87.7%, respectively, in 90 minutes of reaction. Reference [17] sintered a floating MIL88A(Fe)@expanded perlite (M@EP) catalyst, capable of activating H_2O_2, achieving 100% removal of tetracycline antibiotics under low-power artificial UV light and real solar irradiation. The reaction was performed in a continuous bed reactor. Reference [18] synthesized a novel floating Z-scheme photo-Fenton catalyst $FeMo_3O_x$ / gC_3N_4 / EP, where Fe and Mo oxides with mixed valence states and graphitic carbon nitride were loaded onto expanded perlite. The removal efficiencies of tetracycline, oxytetracycline, and chlortetracycline were 98%, 93.1%, and 97.1%, respectively, after 60 minutes of dark adsorption and 60 minutes of photo-Fenton reaction. Reference [19] utilized perlite as a support for a floating TiO2/Fe catalyst in a photo-Fenton reaction. Using 2.77 g/L of this catalyst, complete removal of 1-butyl-2,3-dimethylimidazolium chloride and approximately 80% degradation of TOC and COD were achieved after 4 hours of reaction. The catalyst exhibited reusability after 5 cycles.

II. EXPERIMENTAL

A. MATERIALS

Expanded perlite samples were supplied by Global Minérios. The reagents used in the catalyst synthesis and experimental tests, such as Ferrous sulfate ($FeSO_4.7H_2O$), sodium hydroxide (NaOH), Sulfuric acid (H_2SO_4), and Rhodamine B dye were

supplied by Labsynth, all analytical grade and used without further purification. Hydrogen peroxide (H_2O_2) (35%, w/w) is a commercial solution (35%) acquired from Coremal S.A.

B. CATALYST SYNTHESIS

Initially, the raw perlite was washed several times with distilled water to remove impurities and dried at 105 °C for 24 hours to remove moisture content. A portion of this material was set aside for adsorption and catalysis experiments, and it was designated as PB. The other portion was used in the catalyst synthesis, designated as PB_Fe. The synthesis was performed according to the procedure: 2 g of perlite was added to 200 mL of an aqueous solution of ferrous sulfate heptahydrate ($FeSO_4.7H_2O$) 2% (m/m). The dispersion was stirred for 2 hours in a closed 250 mL Erlenmeyer glass flask at 300 rpm to adsorb the Fe ions on the surface of the perlite. The perlite was dried in an oven for 1 hour at 105 °C before being subjected to an additional heat treatment in a muffle furnace for 3 hours at 280 °C [20]. Figure 3 shows the scheme of the experimental apparatus and procedure used in the synthesis of the catalyst.

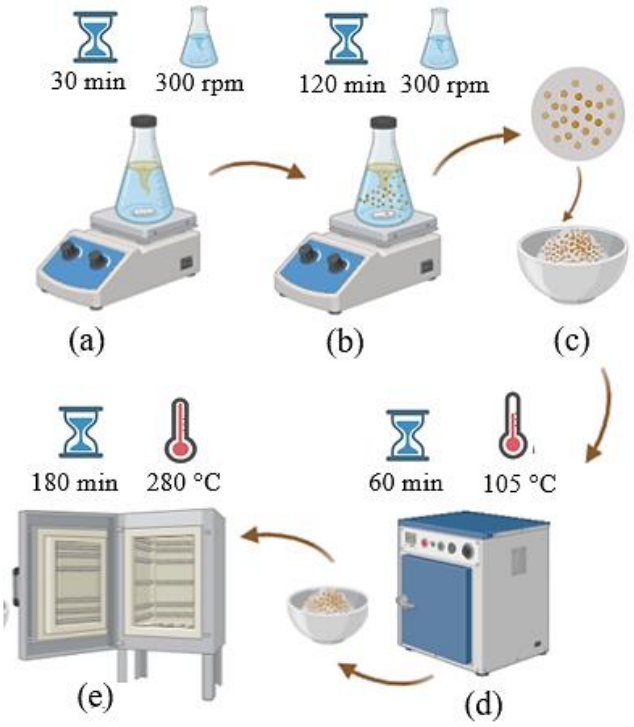

Fig. 3. Synthesis of the catalyst.

C. CHARACTERIZATION

The crystallinity of the catalyst was analyzed by powder X-ray diffraction (PXRD) performed in transmission geometry, on a conventional STADI-P diffractometer (Stoe®, Darmstadt, Germany) operating at 40 kV and 40 mA and equipped with a Ge(111) primary beam monochromator, providing AgKα1 radiation (λ = 0.55941 Å). The powdered samples were deposited between two sheets of cellulose acetate and the sample holder was kept spinning during data collection, and the integrated intensities were recorded by a Mythen 1K linear detector (Dectris®, Baden, Switzerland). To identify the iron oxide phases of the materials, molecular absorption spectra were obtained in the ultraviolet and visible (UV-vis) regions in diffuse reflectance mode (range: 200 nm to 800 nm). UV-vis spectra were recorded on a UV-Visible-NIR Spectrophotometer, Shimadzu (model: UV-3600). To assess iron fixation on perlite and detect alterations in the surface of the support/catalyst, samples of raw perlite, iron-doped perlite before and after Fenton reactions, adsorption tests, and reactions with raw perlite at different pH values were subjected to Fourier Transform Infrared Spectroscopy (FTIR) analysis. The objective of this analysis was to obtain information about the vibrational spectra of the compounds present. FTIR analysis was employed to investigate the chemical changes occurring on the surface of the perlite due to iron doping and the Fenton reaction process. The spectra were obtained in the range of 400 to 4000 cm^{-1}, using the FTIR equipment (model FT-IR Spectrum Two, Perkin Elmer), with both transmission and attenuated total reflectance (ATR) modules, at a resolution of 4 cm^{-1}. For each spectrum, an average of 34 scans was taken. To determine the concentration of iron impregnated in perlite, as well as the amount of iron leached during the heterogeneous Fenton reaction, analyses were performed by atomic absorption spectrometry on the High-Resolution Atomic Absorption Spectrophotometer (FAAS), Contra300, Analytic Jena AG.

The morphology and chemical composition of the samples were obtained using Scanning Electron Microscopy-Energy Dispersive X-ray analysis (SEM-EDX, Jeol JSM-6010LA). For better images, the samples were coated with 20 nm of gold (Sputtering Leica EM ACE 200). At least ten chemical composition analyses were acquired for each sample in different regions. An average of the values is displayed.

D. FENTON EXPERIMENTS

Fenton reactions were carried out in Erlenmeyer flasks (125 mL), under constant stirring (150 rpm). Each test employed 600 mg of Fe-doped immobilized perlite in the presence of 600 mg of H_2O_2 (35%v/v), and 100 mL of RhB solution (25 ppm). The effect of parameters such as initial pH, reaction time (minutes), catalyst dosage (grams of catalyst per volume of RhB), and hydrogen peroxide dosage were studied.

For the study of the variation of the initial pH, 100 mL of RhB solution (25 ppm) was regulated to various initial pH (pH 4, 7, 9, 10, 11, and 12) by the addition of NaOH (0.1 M) and/or H_2SO_4 (0.1 M). For the study of reaction time, time varied from 0 to 240 minutes. Up to here, with the best results found for RhB discoloration, the peroxide dosage was reduced, thus the subsequent reaction test was conducted with 100 mL of RhB solution (25 ppm), 600 mg of Fe-doped perlite, and 200 mg of 35% H_2O_2 for 240 minutes. The Figure 4 shows the schematic diagram of the experimental setup.

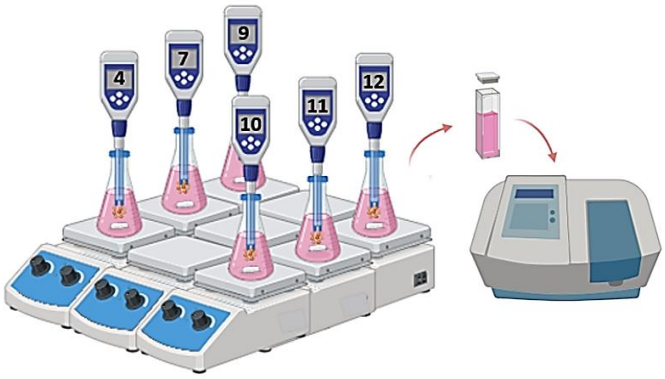

Fig. 4. Experimental Setup, indicating solutions with their respective pH.

E. EXPERIMENTS – RAW PERLITE

In each glass Erlenmeyer flask containing 100 mL of RhB solution, 600 mg of raw perlite was added, to test its adsorption capacity. Tests were carried out at different pH values, namely 4, 7, 11, and 12, adjusted with 1 M NaOH and 0.1 M H_2SO_4. The flasks were placed on a magnetic stirrer, with constant stirring at 150 rpm and a temperature of 25 °C for 120 minutes, according to the representation in Figure 4.
Tests were carried out under the same optimized conditions described in the Fenton reactions item, however, instead of Fe-doped perlite, raw perlite was used to evaluate the influence of the Fe impregnated in the perlite.

F. DEGRADATION TESTS

The efficiency of Rhodamine B removal, evaluated as the discoloration rate of the solution, was calculated from Equation 1. From a 5.2 x 10^{-5} mol.L^{-1} (25 ppm) stock solution of RhB dye, adsorption, and heterogeneous Fenton reaction tests were performed. In all tests, aliquots were withdrawn at 15-minute intervals to evaluate the reaction kinetics.

The removal of Rh B was monitored by the following refer to (1):

$$\%\ RhB\ removal = \frac{[C_{initial}]-[C_{final}]}{[C_{initial}]} * 100 \quad (1)$$

$C_{initial}$ and C_{final} are the initial and final concentrations of the pollutant (RhB) (mg.L^{-1}) and $\%RhB_{removal}$, RhB removal percentagem.

The result of the discoloration of the RhB solution was analyzed in a BEL Engineering spectrophotometer model V-M5, wavelength range 325 nm to 1000 nm, at λ = 554 nm. A calibration curve of RhB solutions, performed in triplicate according to Beer-Lambert's law, was used for the determination of RhB concentration in the samples.

III. RESULTS AND DISCUSSION

A. CATALYSTS CHARACTERIZATION

FTIR

The chemical bonds on the surface of the prepared catalyst were studied by FTIR (Figure 5). The spectra showed four main absorption bands in the raw perlite at 1628 cm^{-1}, 1020 cm^{-1}, 795 cm^{-1} and 559 cm^{-1}. The adsorbed water molecules are represented at 1628 cm^{-1}. The bands at 1020 cm^{-1} and 795 cm^{-1} are attributed to the stretching vibrations of Si-O of Si-O-Si and Si-O-Al, respectively [30], [31]. The synthesized catalyst presented the same peaks as those previously determined in raw perlite, and a new band appears at 559 cm^{-1}, which is related to the presence of iron in the catalyst, indication of the Fe-O-Si bond formation [31]. The adsorption of iron on the porous surface of the perlite occurs through two main mechanisms: physisorption, driven by Van der Waals forces, and chemisorption, which involves the formation of chemical bonds, mainly with the Si–OH groups and the Si–O stretching vibrations [30].

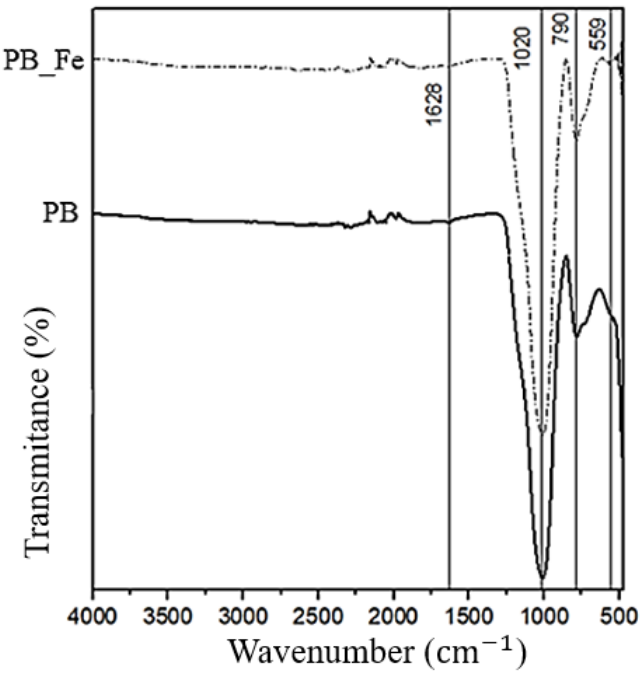

Fig. 5. FTIR Spectra of raw perlite (PB) and synthesized Fe-doped perlite catalyst (PB_Fe).

X-RAY DIFFRACTION (XRD)

X-ray diffraction patterns were measured (Figure 6) to investigate the crystalline nature of the raw perlite (PB) and iron-immobilized perlite (PB_Fe) catalysts, as shown in Fig. 6. The broad peak observed between 15° and 30° indicated the

amorphous nature of perlite. The sharp diffraction peak points to its high degree of structural order and crystallinity [33], [24]. The sharp peak identified at 7.8° for both PB and PB_Fe refers to $(Na,Ca)_{0.3}(A\ell,Mg)_2Si_4O_{10}(OH)_2.nH_2O$, resembling structures found in montmorillonite clay (RRUFF ID: R110052), corroborating the composition of perlite, as presented in the SEM-EDX characterization (Figures 7 and 8). Comparing PB and PB_Fe, it is observed that the synthesized catalyst exhibits four diffraction peaks at 15°, 16°, 17°, 18°, and 21° (2Θ) and a new amorphous hump between 38° and 45°, confirming the efficient incorporation of iron on the crystalline surface of the synthesized catalysts [30], [25]. The peaks at 16°, 17° and 21° coincide with the diffractogram of the goethite mineral (FeO(OH)) (RRUFF ID: R120086). The peak 15° refers to lepidocrocite mineral (FeO(OH)) (RRUFF ID: R050454).

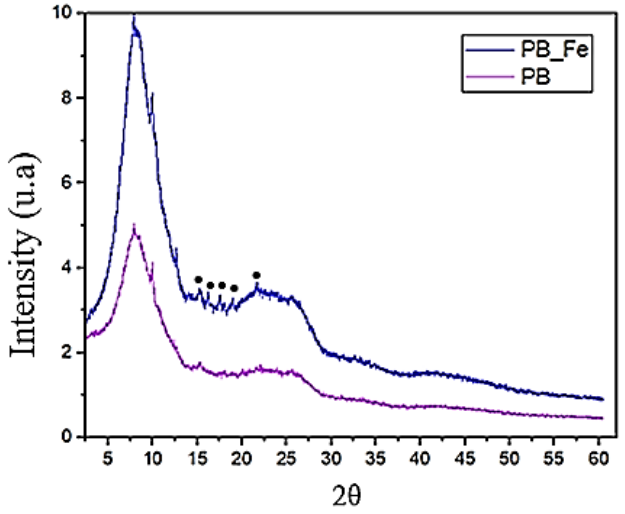

Fig. 6. X-ray diffraction patterns of raw perlite (PB) and Synthesized Catalyst (PB_Fe).

DRS

Diffuse reflectance (DR) spectroscopy were measured (Figure 7) to investigate the identifying the type of iron oxide. The catalyst sample shows absorption bands at approximately 300 - 360 nm. These bands are clearly related to the iron species present in the catalyst. The absorption band at 300 – 360 nm, associated with the bond field electronic transitions of Fe(III) ions in FeOOH due to the coupling of adjacent Fe(III) cations in the structure of this oxyhydroxide [26].

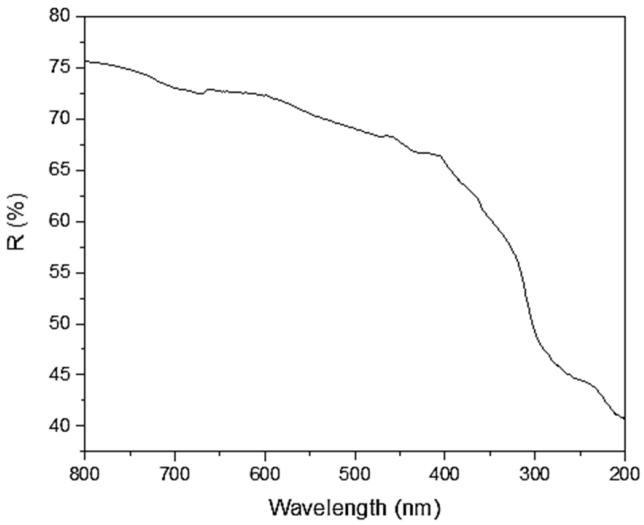

Fig. 7. UV-vis diffuse reflectance spectra of synthesized catalyst (PB_Fe).

SEM-EDX

The surface morphology of pure perlite and modified perlite was studied by SEM technique. Figure 8 (a) shows the SEM image of the raw perlite (PB), presenting a material with lamellar characteristics. Figure 8 (b-g) represents the energy dispersive spectroscopy (EDX) spectra of raw perlite (PB), indicating the distribution of the elements Si, Al, O, Fe, K, Na, the main components of expanded perlite. It is observed that there is an overlap between the elements and that there is a uniform distribution over the material's surface. Among the elements, Fe is present in the lowest percentage, as observed in the image and confirmed in Table I. The major composition of the perlite comprises Si and Al oxides, which was expected, since perlite refers to an aluminosilicate of natural origin, previously reported [27], [28].

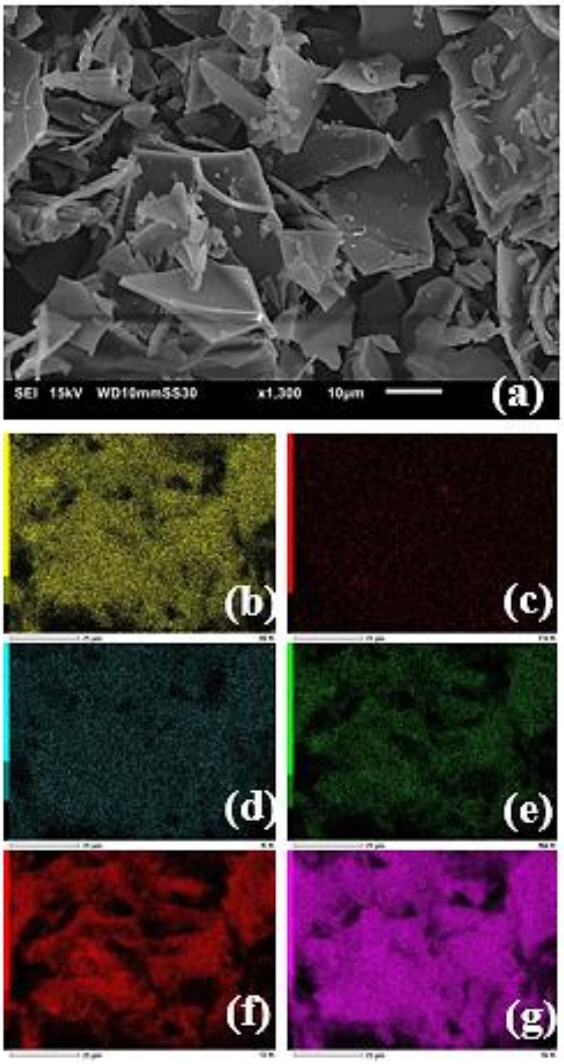

Fig. 8. SEM-EDX raw perlite. (a) Image of raw perlite; (b) Aℓ; (c) Fe; (d) K; (e) Na; (f) O; (g) Si.

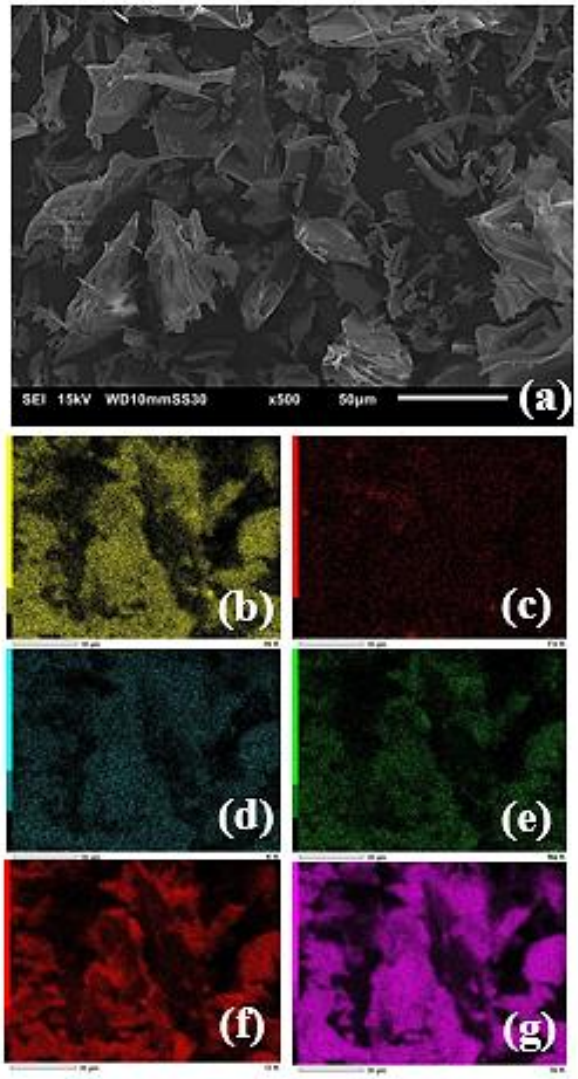

Fig. 9. SEM-EDX Fe-doped perlite. (a) Image of catalyst (PB_Fe); (b) Aℓ; (c) Fe; (d) K; (e) Na; (f) O; (g) Si.

Figure 9 (a) shows the SEM image of the catalyst (PB_Fe), presenting a lamellar material without morphological alterations after iron impregnation. Figure 9 (b-g) shows the energy dispersive spectroscopy (EDX) spectra of the catalyst (PB_Fe), indicating the distribution of the elements Si, Al, O, Fe, K, Na. The increase of iron on the surface of the catalyst, as well as its uniform distribution, stands out, proving that the technique used for iron impregnation was satisfactory.

The elemental composition of the raw perlite and the catalyst can be verified in Table I and Figure 10, obtained from the EDX technique, reaffirming that the synthesis method for obtaining the catalyst was satisfactory, given by the percentage increase in iron from 2.5 to 6.6%.

TABLE I
ELEMENTAL ANALYSIS OF RAW PERLITE AND FE-DOPED PERLITE.

	PB	PB_Fe
Element	% Elementar	
Aℓ	12.51	12.37
Fe	2.50	6.60
K	11.65	10.13
Na	4.89	5.07
Si	68.45	65.83

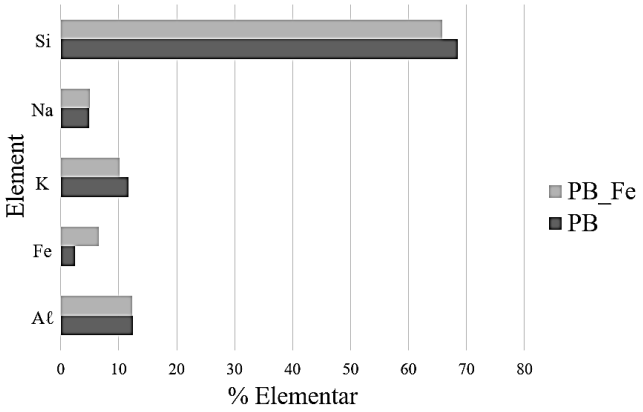

Fig. 10. Elemental analysis comparison of raw and Fe-doped perlite.

B. FENTON EXPERIMENTS

According to Figure 11, the removal of RhB by heterogeneous Fenton reaction using 600 mg of catalyst (PB_Fe) and 600 mg of 35% H_2O_2 showed a removal % of around 50% in the first fifteen minutes of the reaction. Reactions that occurred at pH 4, 11, and 12 obtained higher RhB removal percentages than at pH 7, 9, and 10. Considering 150 minutes of reaction, the RhB removals at pH 4, 7, 9, 10, and 11 were, respectively, 96.9%; 56.4%; 66.6%; 70.9%, and 92.1%. For pH 12, 99.6% RhB removal was achieved in 110 minutes of reaction.

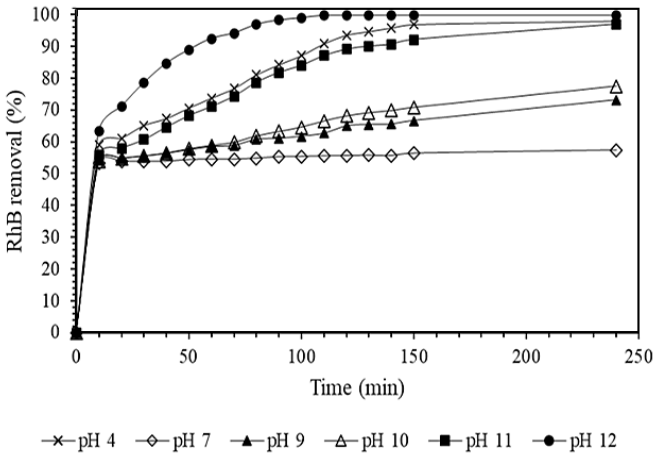

Fig. 11. Effect of pH on RhB removal

Considering that expanded perlite is a porous material, the removal of Rhodamine B is attributed not only to reaction mechanisms arising from radical generation but also to the adsorption of the organic compound molecules in the pores of the material. Perlite has Fe in its composition, however, in a low percentage, providing a low amount of active sites available for radical formation. Therefore, it was necessary to carry out tests with raw perlite (PB), in the absence of peroxide, to evaluate the capacity of Rhodamine B removal by adsorption.

To this end, experiments were conducted to evaluate the capacity of dye removal by adsorption mechanism on raw perlite, at different pH values. Figure 12 presents the results of removal by adsorption, comparing them to the results of removal by Fenton reaction.

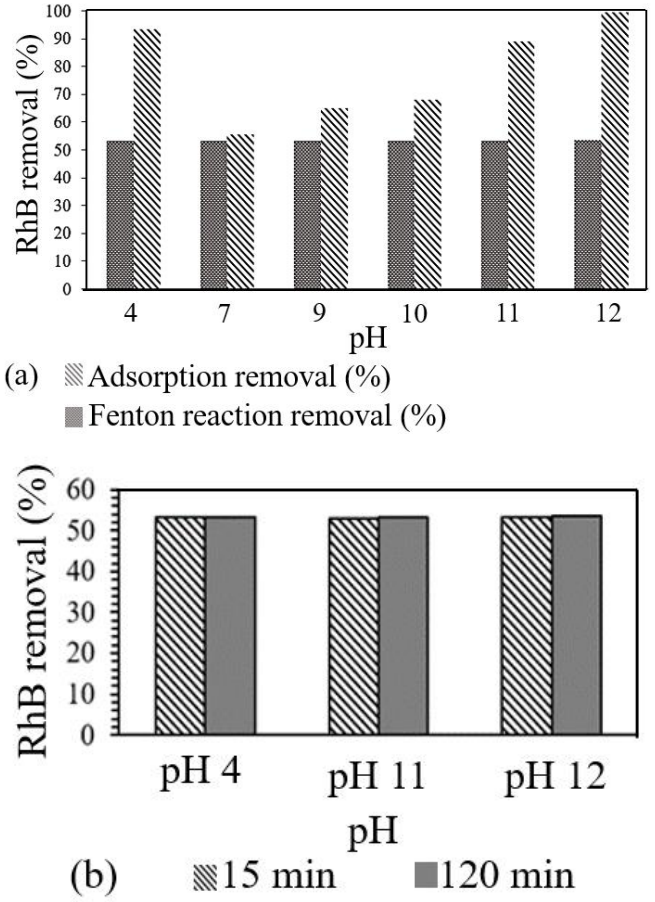

Fig. 12. (a) Comparison between RhB removal by adsorption and heterogeneous Fenton reaction; (b) Adsorption removal at 15 and 120 min.

As shown in Figure 12 (a), the removal of RhB by adsorption, using 600 mg of raw perlite (PB), showed a removal rate close to 53%. As the RhB removal results by Fenton reaction at pH 4, 11, and 12 were significantly higher than the other results, these data were highlighted in Figure 12 (b), showing that the removals were achieved during the initial fifteen minutes, stabilized over 2 hours, indicating that it is independent of the pH, as shown in Figure 12 (a) and (b).

With the best results obtained in this first phase, being these reactions conducted at pH 4, 11, and 12, new experiments were carried out, keeping the amount of catalyst, pH, reaction volume, and RhB concentration constant, reducing the amount of H_2O_2 to 200 mg. The reduction of the peroxide dosage was carried out to obtain more economical conditions for the RhB removal process. Reactions conducted with excess peroxide can decrease the efficiency of removal of organic compounds, given that the Fenton reaction comprises a mechanism that starts with Fe^{2+} present in the catalyst, breaking down H_2O_2 into hydroxyl radical (•OH) and anion, hydroxyl (OH^-). Iron recycles between the +2 and +3 oxidation states. Fe^{3+} reacts with H_2O_2 producing hydroperoxyl radical ($HO_2^{\bullet}$). This radical can reduce the Fe^{3+} ion to Fe^{2+}, but contributes little to organic mineralization

because it has low oxidizing power (E° = 1.65 V), very similar to H_2O_2 (E° = 1.78 V), that is, the rate of oxidation of organic matter by $HO_2^{\bullet}$ is lower than that of the •OH radical. Given these mechanisms, an adequate dosage of peroxide is necessary to avoid spending on reagents that are not reused during the process, as well as to promote an improvement in reaction yield [7], [32]. The reactions carried out with the low H_2O_2 dosage peroxide dosage presented, for pH 4 and 11, the removal percentage of 95.8% and 90.2%, respectively, in 150 minutes of reaction. Under the same conditions, for pH 12, the removal percentage was 98.6% in 105 minutes. These results are presented in Fig. 13. The results obtained with reactions performed with 200 mg of peroxide were slightly better than those found with reactions performed with 600 mg of peroxide. The differences in removal percentages were not relevant, but the savings in reagents became preponderant in determining operating conditions. It is worth noting that the RhB removal reaction occurred in both acidic and basic media, indicating that the catalyst prepared overcame restricted pH ranges (2-4) applied to homogeneous Fenton-type reactions. This characteristic is attributed to the iron cations being under the influence of a strong electrostatic field in the structure of raw perlite. Satisfactory impregnation of iron onto the support inhibits the formation of iron hydroxide, a common route when operating in alkaline media [32], [33].

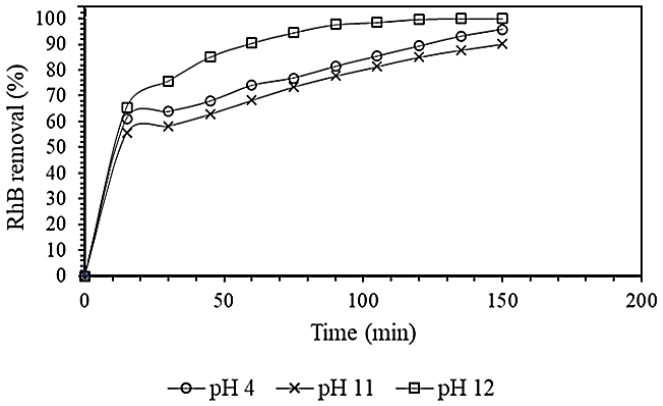

Fig. 13. RhB removal by heterogeneous Fenton reaction using 600 mg of catalyst (PB_Fe) and 200 mg of H_2O_2.

In order to prove the activity of the impregnated iron, reactions were carried out substituting the catalyst (PB_Fe) with raw perlite (PB). The RhB removals by reaction between 600 mg of raw perlite (PB) and 200 mg of 35% H_2O_2 are shown in Figure 14. It is observed that there was no removal of RhB in an acidic medium, presenting a result close to that observed in the adsorption mechanism (Figure 12 a). In alkaline conditions, a RhB removal of around 72% at pH 11 and 90% at pH 12 was obtained in 120 minutes of reaction. During the initial fifteen minutes, there was a removal percentage greater than 50% for both acidic and alkaline reaction media.

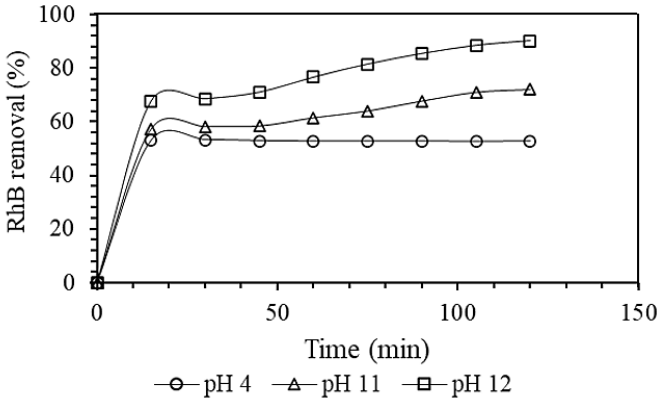

Fig. 14. RhB removal by reaction between raw perlite (PB) and H_2O_2.

A comparison was established between different methods of RhB removal by Fenton reaction at different pH values, also comparing removals by adsorption and reaction with raw perlite, as shown in Figure 15.

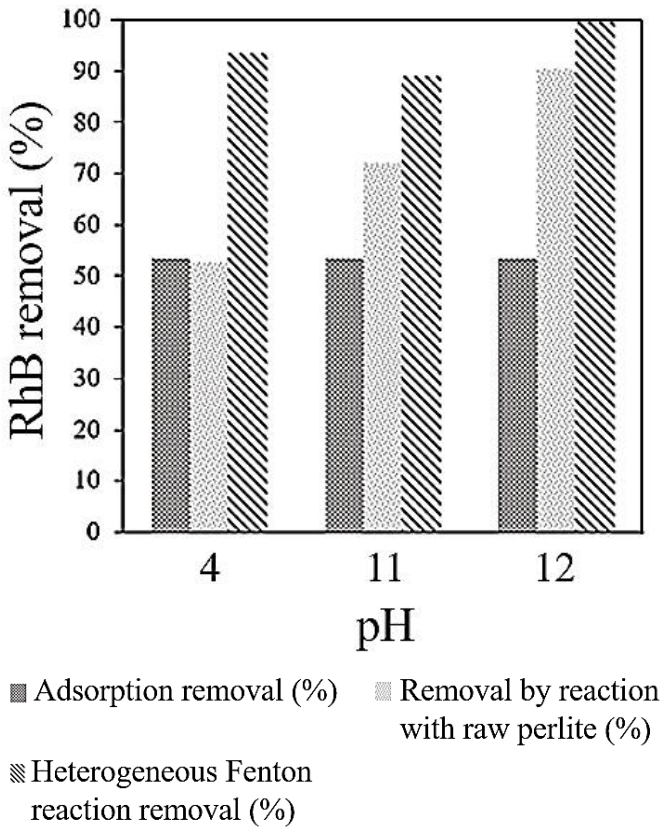

Fig. 15. Comparison of RhB removal methods by adsorption, reaction of raw perlite with 200 mg of H_2O_2, and heterogeneous Fenton reaction with 200 mg of H_2O_2.

Figures 16, 17 and 18 presents a comparison between the methods of RhB removal (adsorption, Fenton reaction with catalyst PB_Fe and reaction with raw perlite PB), as a function of time, for pH 4, 11 and 12. For alkaline conditions, Figure 17 and 18, it is observed that there is RhB removal even when the catalyst (PB_Fe) is replaced by raw perlite (PB), with a significant increase when comparing pH 11 with pH 12, with

pH 12 showing approximately 10% more RhB removal than at pH 11. In acidic conditions, Figure 16, there is an equalization between the results obtained between the removal processes by adsorption and by reaction with raw perlite (PB). In all cases, removal results exceeding 50% are observed in time exceeding 15 minutes.

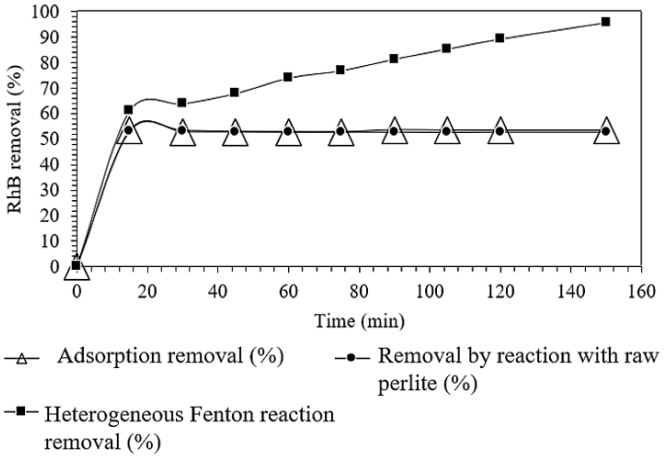

Fig. 16. A comparative study of RhB removal methods at pH 4.

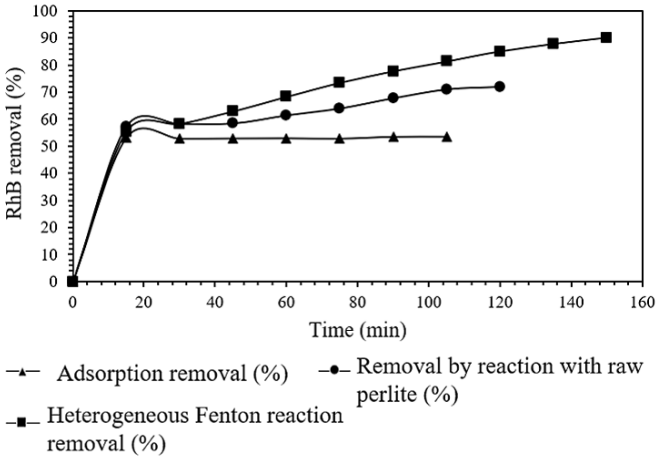

Fig. 17. A comparative study of RhB removal methods at pH 11.

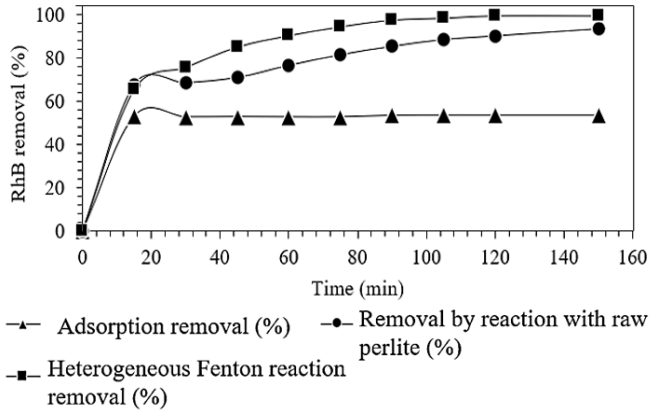

Fig. 18. A comparative study of RhB removal methods at pH 12.

FAAS

To determine the percentage of residual iron after the reactions, atomic absorption spectrometry analysis with a flame (FAAS) was performed, following the experimental protocol described in the methodology. This procedure aimed to investigate the occurrence of iron leaching throughout the reaction process. It was observed that the leaching percentages of Fe under acidic conditions (pH 4) and alkaline conditions (pH 11 and pH 12) were 36.1%, 14.9%, and 29.8%, respectively. The pH of a solution has a significant impact on the solubility of metals. In the case of Fenton reactions, the ideal pH should be around 3, as pH 3 contributes to a higher concentration of ferrous and ferric ions in solution compared to other pH values. For instance, a ferric ion added to a solution with pH 3 exists as $Fe(H_2O)_6^{3+}$. This hexa-aqua ferric complex undergoes further hydrolysis and forms other complexes (Refer to 2 and 3). A hydrated metal complex loses protons as pH increases, forming hydroxylated species; in other words, a pH greater than 3 increases the concentration of complexes other than $Fe(H_2O)_6^{3+}$. Consequently, the useful fraction of ferric ions for the Fenton process decreases with increasing pH values due to the precipitation of the catalyst [29].

$$[Fe(H_2O)_6]^{3+} + H_2O \rightarrow [Fe(OH)(H_2O)_5]^{2+} + H_3O^+ \quad (2)$$

$$[Fe(OH)(H_2O)_5]^{2+} + H_2O \rightarrow [Fe(OH)_2(H_2O)_4]^{+} + H_3O^+ \quad (3)$$

In an alkaline environment, the decomposition of H_2O_2 generates HO_2^- ions, as shown in Refer to (4). These ions react with H_2O_2 to generate free radicals according Refer to (5). Subsequently, OH^- ions attack the Fe-O bonds on the catalyst surface, leading to their cleavage and the release of Fe(III) into the solution. HO_2^- reduces Fe^{3+} to Fe^{2+}, producing the hydroperoxyl radical ($\bullet O_2H$) (Refer to (6)). In solution, Fe^{3+}/Fe^{2+} undergoes a Fenton-like reaction with H_2O_2, generating $\bullet OH$ and $\bullet O_2H$ as Refer to (7) and (8). It is important to highlight that $\bullet O_2^-$ is the basic conjugate form of $\bullet O_2H$ in an alkaline environment according Refer to (9) and (10) [30].

$$H_2O_2 + OH^- \rightarrow HO_2^- + H_2O \quad (4)$$

$$H_2O_2 + HO_2^- \rightarrow \bullet O_2H + \bullet OH + OH^- \quad (5)$$

$$Fe^{3+} + HO_2^- \rightarrow Fe^{2+} + \bullet O_2H \quad (6)$$

$$Fe^{2+} + H_2O_2 \rightarrow Fe^{3+} + \bullet OH + OH^- \quad (7)$$

$$Fe^{3+} + H_2O_2 \rightarrow Fe^{2+} + \bullet O_2H + H^+ \quad (8)$$

$$H_2O_2 + \bullet OH \rightarrow \bullet O_2H + H_2O \quad (9)$$

$$\bullet O_2H + OH^- \rightarrow \bullet O_2^- + H_2O \quad (10)$$

As described in the homogeneous Fenton reaction mechanism, the solubility of Fe in acidic media is high. Therefore, it cannot be disregarded that Fe leaching from the catalyst occurs under acidic conditions for heterogeneous Fenton. These leached Fe ions can initiate the degradation reaction via a homogeneous Fenton mechanism. A heterogeneous Fenton reaction, occasionally, may occur in two stages, comprising a first slow induction phase, characterized by a heterogeneous Fenton mechanism and slow Fe ion leaching from the surface, and a

second phase, represented by the homogeneous Fenton mechanism, originating from the leached Fe ions. Such a mechanism is described as a homogeneous reaction induced by a heterogeneous reaction [30].

When comparing the heterogeneous Fenton reactions carried out at different pH values, it is observed that both in alkaline and acidic media, the same percentages of dye removal are achieved. However, in alkaline media, these removal percentages are reached in a shorter period. Such differences can be attributed to the formation of more than one type of radical, besides hydroxyl (•OH), the superoxide anion ($O_2^{-\bullet}$). Reference [30] evaluated the degradation of Rhodamine B dye from the generation of superoxide anion radicals ($O_2^{-\bullet}$) in an aqueous $NaOH/H_2O_2$ medium at room temperature. In this process, NaOH is regenerated while H_2O_2 is consumed, according refer to (11) at (14):

$$2NaOH + H_2O_2 \rightarrow Na_2O_2 + 2H_2O \quad (11)$$
$$Na_2O_2 + 2H_2O_2 \rightarrow 2NaO_2 + 2H_2O \quad (12)$$
$$NaO_2 \rightarrow Na+ + O_2^{-\bullet} \quad (13)$$
$$RhB + 2NaO_2 + H_2O \rightarrow \text{Intermediate/mineralized products} + CO_2 + 2NaOH \quad (14)$$

According to the authors, the $NaOH/H_2O_2$ process has the characteristic of sequestering CO_2 produced during the mineralization of pollutant species, according refer to (15):

$$CO_2 + 2NaO_2 \rightarrow Na_2CO_3 + 1.5O_2 \quad (15)$$

An increase in bubble formation in the reaction system was observed during the experiments. It is estimated that the NaO_2 species that is not participating in the degradation process may have an interaction with any dissolved organic matter, producing molecular O_2 [31]. Rhodamine B removal tests were carried out under alkaline conditions (pH 11 and 12), in the absence of a catalyst, with the addition of hydrogen peroxide (600 and 200 mg) in order to verify the contribution of the radicals formed by the previously proposed mechanism. At pH 11, adding 600 and 200 mg of H_2O_2 35%, 11 and 3.5% removal of rhodamine B, respectively, were obtained. At pH 12, adding 600 and 200 mg of H_2O_2 35% resulted in 14 and 4.5% removal of rhodamine B, respectively. The same test was carried out in acidic conditions (pH 4), with no removal of rhodamine B, regardless of the amount of $3H_2O_2$ 35% added.

C. EVALUATION OF THE CATALYST AFTER REACTION

The iron content was determined by Flame Atomic Absorption Spectrometry (FAAS). It was found that after the first cycle, there was a leaching of approximately 30% (mass) of iron to the fluid phase of the reaction medium, both in acidic and alkaline conditions. It was also analyzed whether there were morphological changes on the surface of the catalyst after reactions under acidic and alkaline conditions (pH 4 and 11, respectively), as well as whether there was any modification in the distribution of iron for both conditions. The results of the SEM-EDX analyses are shown in Figures. 19 and 20, for acidic and alkaline conditions, respectively.

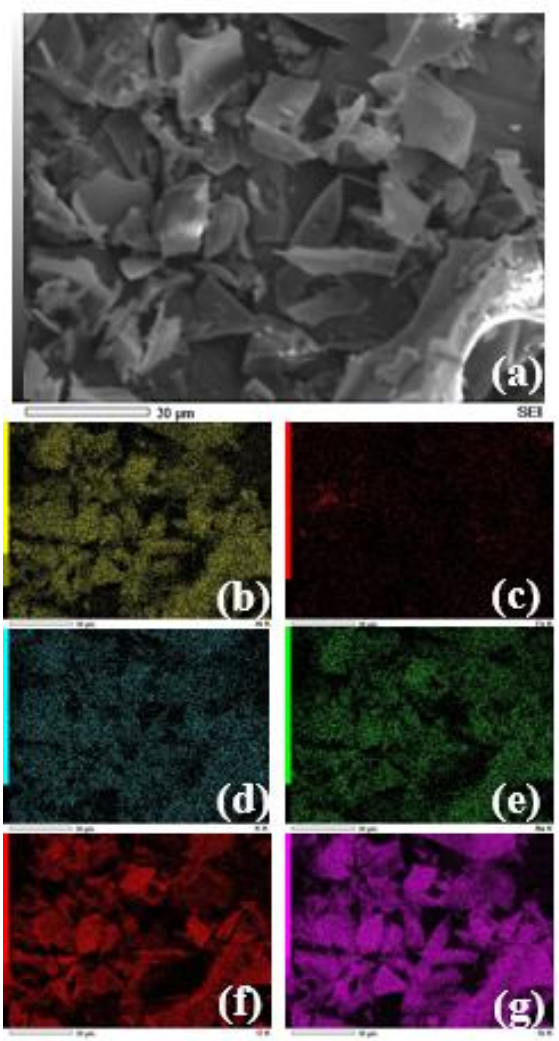

Fig. 19. SEM-EDX of the catalyst after reaction at pH 4. (a) Image of catalyst after reaction; (b) Aℓ; (c) Fe; (d) K; (e) Na; (f) O; (g) Si.

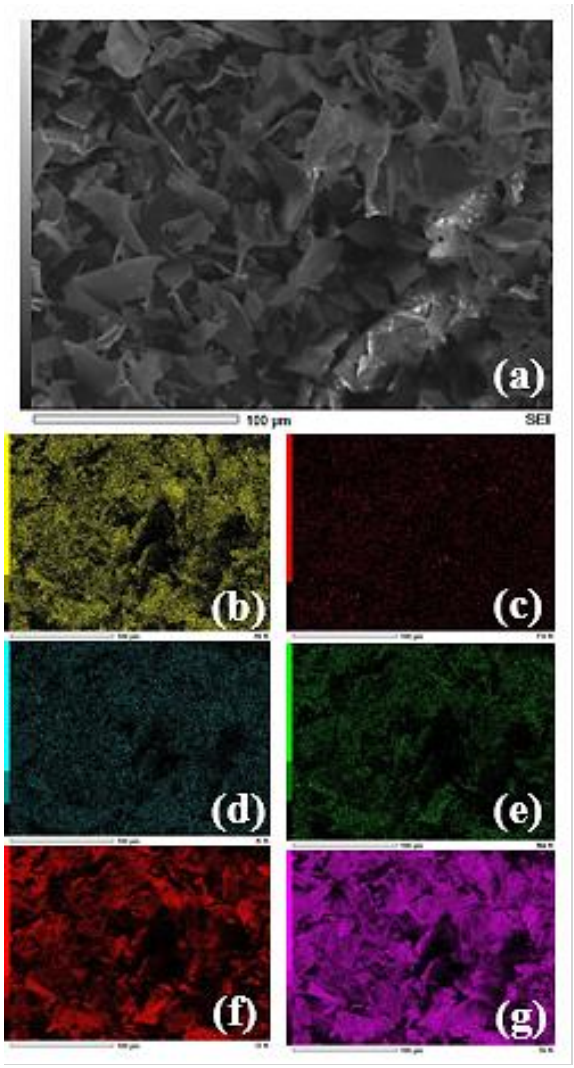

Fig. 20. SEM-EDX of the catalyst after reaction at pH 11. (a) Image of catalyst after reaction; (b) Aℓ; (c) Fe; (d) K; (e) Na; (f) O; (g) Si.

TABLE II
ELEMENTAL ANALYSIS OF Fe-DOPED PERLITE AFTER REACTION AT pH 4 AND pH 11

	PB_Fe Catalyst after reaction at pH 4	PB_Fe Catalyst after reaction at pH 11
Element	% Elementar	
Aℓ	12.49	11.94
Fe	5.60	6.16
K	11.06	11.11
Na	4.89	5.02
Si	65.95	65.35

Table II shows the elemental composition of the catalysts after their use at pH 4 and 11. It is noted that in an acidic medium, there was a higher percentage reduction in iron than that observed in an alkaline medium. This result corroborates the fact that a heterogeneous Fenton system can generate the •OH radical by two distinct methods: by the heterogeneous catalytic mechanism itself or through the homogeneous Fenton reaction, which can be triggered by the leaching of iron from the solid catalyst. The presence of leached iron from the solid catalyst can increase the reaction rate via the homogeneous Fenton pathway; however, continuous leaching of metal ions results in the deactivation of the heterogeneous catalyst. Furthermore, the leaching of metal ions from a catalyst is also influenced by the pH of the solution, and for iron, this leaching is more common under acidic conditions. However, the catalyst still showed activity after three cycles of use, attributing this leaching to the first cycle of use conditions, arising from possible excesses of iron that were not removed during the washing of the catalyst before its first use. Between cycles, the catalyst was washed with distilled water several times and dried at 100 °C for 4 hours. The removal efficiency between cycles was reduced by 20% between the first and second cycle and reduced by 10% between the second and third cycle.

IV. CONCLUSION

According to the findings, the Fe impregnation method on perlite mineral was satisfactory, and the catalyst could be reused with low leaching rates in subsequent cycles, as confirmed by the results. Further investigations are necessary regarding its recycling to maintain its catalytic activity, as well as synthesis evaluations to enhance the stability of Fe on the perlite. The porous structure of perlite allowed the removal of Rhodamine B dye through a combined mechanism involving Fenton reaction and adsorption, and its porosity was crucial for the immobilization of iron on its surface. The synthesized catalyst showed advantages by operating in a wide pH range and being easily separated from the reaction medium. The applied heterogeneous Fenton reaction method is promising for applications in scaled-up systems for Rhodamina B removal, given the ease of separating the catalyst from the reaction medium, which has the characteristic of flotation, eliminating the need for costly separation methods such as centrifugation or filtration.

V. ACKNOWLEDGEMENTS

The authors of this work acknowledge the São Paulo Research Foundation (FAPESP Processes: 2021/09775-1, 2023/08875-8, 2023/17516-1 and 2023/01634-5), the CAPES/UFABC, the Multiuser Experimental Centers of UFABC (CEMs/UFABC) and the National Service for Industrial Apprenticeship (SENAI).

VI. CONFLICTS OF INTEREST

The authors declare no conflict of interest.

VII. REFERENCES

[1] RANI, M; SHANKER, U. Insight in to sunlight-driven rapid photocatalytic degradation of organic dyes by hexacyanoferrate-based nanoparticles. Enviromental Science

and Pollution Research, v. 28, p. 5637 – 5650, 2021. DOI: https://doi.org/10.1007/s11356-020-10925-7.

[2] AL-GHEETHI, A. A; AZHAR, Q. M; KUMAR, P. S; YUSUF, A. A; AL-BURIAHI, A. K; MOHAMED, R. M. S. R; AL-SHAIBANI, M. M. Sustainable approaches for removing Rhodamine B dye using agricultural waste adsorbents: A review. Chemosphere, 287, 132080, 2022. DOI: 10.1016/j.chemosphere.2021.132080.

[3] MOHOD, A. V; MOMOTKO, M; SHAH, N. S; MARCHEL, M; IMRAN, M; KONG, L; BOCZKAJ, G. Degradation of Rhodamine dyes by Advanced Oxidation Processes (AOPs) – Focus on cavitation and photocatalysis - A critical review. Water Resources and Industry, v. 30, 100220, 2023. DOI: https://doi.org/10.1016/j.wri.2023.100220.

[4] YUSUF, T. L; ORIMOLADE, B. O; MASEKELA, D; MANBA, B; MABUBA, N. The application of photoelectrocatalysis in the degradation of rhodamine B in aqueous solutions: a review. Royal Society of Chemistry Advances, 12, 26176, 2022. DOI: https://doi.org/10.1039/D2RA04236C.

[5] MOKHBI, Y; KORICHI M; AKCHICHE Z. Combined photocatalytic and Fenton oxidation for oily wastewater treatment. Applied Water Science, 2019. DOI: https://doi.org/10.1007/s13201-019-0916-x.

[6] ZHANG, J; YAN, M; SUN, G; LI, X; HAO, B; LIU, K. Mg–Fe–Al–O spinel: Preparation and application as a heterogeneous photo-Fenton catalyst for degrading Rhodamine B. Chemosphere, v. 304, 135318, 2022. DOI: 10.1016/j.chemosphere.2022.135318.

[7] BRILLAS, E. Fenton, photo-Fenton, electro-Fenton, and their combined treatments for the removal of insecticides from waters and soils. A review. Separation and Purification Technology, 284, 120290, 2022. DOI: https://doi.org/10.1016/j.seppur.2021.120290.

[8] KARIMI, S; YARAKI, M. T; KARRI, R. R. A comprehensive review of the adsorption mechanisms and factors influencing the adsorption process from the perspective of bioethanol dehydration. Renewable and Sustainable Energy Reviews, v. 107, p. 535-553, 2019. DOI: 10.1016/j.rser.2019.03.025.

[9] SHEN, Y; XIAO, Y; ZHANG, H; HONGIJE, F; LI, Y; YAN, Z; ZHANG, W. Synthesis of magnetic biochar-supported Fe-Cu bimetallic catalyst from pulp and paper mill wastes for the Fenton-like removal of rhodamine B dye. Chemical Engineering Journal, 477, 146823, 2023. Doi: 10.1016/j.cej.2023.146823.

[10] SUN, L; SHEN, X; ZHANG, H; PANG, Y. Amino-functionalized iron-based MOFs for Rhodamine B degradation in heterogeneous photo-Fenton system. Journal of Photochemistry and Photobiology A: Chemistry, 452, 115544, 2024. Doi: 10.1016/j.jphotochem.2024.115544.

[11] XU, Q; XUE, Q; TAN, S; CHENG, Z; QI, X; YAN, C. Enhanced photo-Fenton degradation of dyes under visible light with recyclable γ-Fe2O3/CQDs: Catalyst preparation, performance and mechanism insight. Environmental Pollution, 347, 123634, 2024. Doi: 10.1016/j.envpol.2024.123634.

[12] XU, M; TIAN, Q; QUAN, Y; XU, L; NAMADCHIAN M. Preparation of a New and Effective Heterogeneous Catalyst for Treatment of Organic Pollutant Using Fenton Process. Topics in Catalysis, 2024. Doi: 10.1007/s11244-024-01959-z.

[13] ZHOU, P; YANG, W; LU, T; RU, X; DAI, Z; OFORI, M. A; HOU, J. Heterogeneous Fenton for Removal Rhodamine-B by Iron-bearing Attapulgite Granular Catalysts. Water, Air, Soil Pollution, 234, 61, 2023. Doi: 10.1007/s11270-023-06081-6.

[14] KASAI, M; KOBAYASHI, Y; TOGO, M; NAKAHIRA, A. Synthesis of zeolite-surface-modified perlite and their heavy metal adsorption capability. Science Direct, Materials Today: Proceedings, v. 16 p. 232-238, 2019. DOI: https://doi.org/10.1016/j.matpr.2019.05.247.

[15] JIANG, L; WANG, J; WU, X; ZHANG, G. A Stable Fe2O3/Expanded Perlite Composite Catalyst for Degradation of Rhodamine B in Heterogeneous Photo-Fenton System. Water Air Soil Pollut, v.228, n. 463, 2017. DOI: 10.1007/s11270-017-3646-4.

[16] SARESHKEH, A. T; RASOULIFARD, M. H; ABID, A; DORRAJI, M. S. S; HOSSEINI, S. F. Exploiting the efficiency of narrow band gap S-doped g-C3N4/Expanded Perlite/Red Ocher nanocomposite for high-level eliminating halogenated dye in Cool-White-SMD/H2O2 system. Journal of Alloys and Compounds, 1005, 175822, 2024. Doi: 10.1016/j.jallcom.2024.175822.

[17] LIU, G; YI, X; CHU, H; WANG, C; GAO, Y; WANG, F; WANG, F; WANG, P; WANG, J. Floating MIL-88A(Fe)@expanded perlites catalyst for continuous photo-Fenton degradation toward tetracyclines under artificial light and real solar light. Journal of Hazardous Materials, 472, 134420, 2024. Doi: 10.1016/j.jhazmat.2024.134420.

[18] LIU, Y; WANG, X; SUN, Q; YUAN, M; SUN, Z; XIA, S; ZHAO, J. Enhanced visible light photo-Fenton-like degradation of tetracyclines by expanded perlite supported FeMo3Ox/g-C3N4 floating Z-scheme catalyst. Journal of Hazardous Materials, 424, 127387, 2022. Doi: 10.1016/j.jhazmat.2021.127387.

[19] DÍEZ, A. M; PAZOS, M; SANROMÁN, M. A. Bifunctional floating catalyst for enhancing the synergistic effect of LED-photolysis and electro-Fenton process. Separation and Purification Technology, 230, 115880, 2020. Doi: 10.1016/j.seppur.2019.115880.

[20] BOUMNIJEL, I; Hamdi, N; HACHEM, H; AMOR H. B; MIHOUBI, D. Fenton oxidation catalysed by heterogeneous iron–perlite for 8-hydroxyquinoline-5-sulfonic acid (8-HQS) degradation: efficiency comparison using raw and calcined perlite as precursors for iron fixation. Environmental Science and Pollution Research, v. 30, p. 6201 – 6215, 2023. DOI: 10.1007/s11356-022-22619-3.

[21] ESMAIELPOUR, M; AKHLAGHINIA, B; JAHANSHAHI, R. Green and efficient synthesis of aryl/alkylbis(indolyl)methanes using Expanded Perlite-PPA as a heterogeneous solid acid catalyst in aqueous media. Journal Chemistry Science, v. 129, n. 3, p. 313-328, 2017. DOI: 10.1007/s12039-017-1246-x.

[22] PUGA, A; ROSALES, E; PAZOS, M; SANROMÁN, M. A. Prompt removal of antibiotic by adsorption/electro-Fenton degradation using an iron-doped perlite as heterogeneous catalyst. Process Safety and Environmental Protection, v. 144, p. 100-110, 2020. DOI: https://doi.org/10.1016/j.psep.2020.07.021.

[23] AHMED I. M; ATTIA L.A; ATTALLAH M.F. Modification of perlite to prepare low cost zeolite as adsorbent material for removal of ^{144}Ce and $^{152+154}Eu$ from aqueous

solution. Radiochimica Acta, v. 108, n. 9, p. 727–735, 2020. DOI: https://doi.org/10.1515/ract-2019-3221.
[24] SAUFI, H; EL ALOUANI, M; ALEHYEN, S; EL ACHOURI, M; ARIDE, J; TAIBI, M. Photocatalytic Degradation of Methylene Blue from Aqueous Medium onto Perlite-Based Geopolymer. International Journal of Chemical Engineering, 7 pages, 2020. DOI: https://doi.org/10.1155/2020/9498349.
[25] BRINDHA, K; AMUTHA, P; KRISHNAKUMAR, B. et al. BiCl3-modified perlite as an effective catalyst for selective organic transformations: a green protocol. Res Chem Intermed, v. 45, p. 4367–4381, 2019. DOI: 10.1007/s11164-019-03836-x.
[26] AZEVEDO, C. K. S; REIS, E. A; GERMINO, J. C; MORETO, J. A; TEREZO, A. J; QUITES, F. J. New hybrids based on iron (III) oxyhydroxide and gold nanoparticles (AuNPs / FeOOH) as catalysts. Química Nova, v. 40, p. 534-540, 2017. DOI: 10.21577/0100-4042.20170046.
for the reduction of organic environmental pollutants
[27] ESKANDARI, F; BAYAT, M. Perlite-Catalyzed Chemical Fixation of Carbon Dioxide Under Solvent-free and Low-pressure CO_2 Conditions. Silicon, v. 16, p. 3709-3717, 2024. DOI: https://doi.org/10.1007/s12633-024-02956-3.
[28] LAKSHMINARAYANAN, K; SIVANANDHAN, M; RAMASUNDARAM, S; OH, T. H; SHAH, K. J; SARANRAJ, K; PARASURAMAN, A; BALU, K. $NbCl_5$ Functionalized Perlite: A Potent and Recyclable Catalyst for Synthesis of Pyrans. Sustainability, v. 15, p. 3678, 2023. DOI: 10.3390/su15043678.
[29] NIDHEESH, P. V. Heterogeneous Fenton catalysts for the abatement of organic pollutants from aqueous solution: a review. RSC Advances, v. 51, 40552-40577, 2015. DOI: 10.1039/C5RA02023A
[30] WANG, X; BAO, J; ZI, S; LUO, Y; LIU, C; ZENG, Z; WANG, F; YANG, J; SHI, L; LI, K; SUN, X. Insight into NOx removal mechanism by H2O2 activation via MIL-100(Fe) in an alkaline environment. Journal of Environmental Chemical Engineering, v. 12, 113456, 2024. DOI: 10.1016/j.jece.2024.113456.
[31] VERMA, P; SAMANTA, S. K; MISHRA, S. Photon-independent NaOH/H2O2–based degradation of rhodamine-B dye in aqueous medium: Kinetics, and impacts of various inorganic salts, antioxidants, and urea. Journal of Environmental Chemical Engineering, v. 8, p. 103851, 2020. DOI: 10.1016/j.jece.2020.103851.
[32] LIMA, M. F; SILVA, B. G; ASENCIOS, Y. J. Optimization of industrial Fenton process of phenolic effluent using artificial neural network and design of experiments. Chemical Engineering Communications, 2024. DOI: https://doi.org/10.1080/00986445.2024.2351491.
[33] THOMAS, N; DIONYSIOU, D. D; PILLAI, S. C. Heterogeneous Fenton catalysts: A review of recent advances. Journal of Hazardous Materials, v. 404, 124082, 2021. DOI: https://doi.org/10.1016/j.jhazmat.2020.124082.
[34] LUO, H; ZENG, Y; HE, D; PAN, X. Application of iron-based materials in heterogeneous advanced oxidation processes for wastewater treatment: A review. Chemical Engineering Journal, 407, 127191, 2021. DOI: https://doi.org/10.1016/j.cej.2020.127191.
[35] RRUFF Project. Acess date: 14/10/2024: https://rruff.info/.